Phase separation in nematic microemulsions probed by one-dimensional spectroscopic deuteron magnetic resonance microimaging

Andrija Lebar,[1] Zdravko Kutnjak,[1] Hajime Tanaka,[2] Boštjan Zalar,[1,3] and Slobodan Žumer[1,3]
[1]*Jožef Stefan Institute, P.O. Box 3000, 1001 Ljubljana, Slovenia*
[2]*Institute of Industrial Science, University of Tokyo, 4-6-1 Komaba, Meguro-ku, Tokyo 153-8505, Japan*
[3]*Department of Physics, Faculty of Mathematics and Physics, University of Ljubljana, Jadranska 19, 1000 Ljubljana, Slovenia*
(Received 20 December 2007; published 23 September 2008)

We present a study of a phase-transition-driven separation in microemulsions of nanosized lyotropic inverse micelles and thermotropic liquid crystal pentylcyanobiphenyl (5CB) with 5%, 8%, and 15% micelle concentration. Using deuteron nuclear magnetic resonance (DNMR) microimaging in combination with conventional microscopy as well as ac calorimetry, we demonstrate a phase separation scenario in which micelles are expelled from the nematic phase during the I-N conversion. Due to a difference in density the micelle-rich isotropiclike phase spatially separates from the micelle-free nematic phase. A relatively sharp interface, formed between the two phases, can be controllably shifted by temperature-induced conversion between the phases. Once expelled, micelles do not remix into the nematic phase, whereas in the isotropic state their remixing takes place over several days. Temperature dependence of the linewidth of isotropic spectral component has been analyzed in terms of molecular reorientations mediated by translational displacements, assuming isotropically distributed directors of nanosized nematic domains. With our results, the existence of the proposed transparent nematic state cannot be completely ruled out. However, if present, the nematic order in such a phase must be extremely low.

DOI: 10.1103/PhysRevE.78.031707 PACS number(s): 61.30.−v, 68.05.Gh

I. INTRODUCTION

Mixtures of anisotropic fluids with various types of colloidal particles have in recent years been extensively investigated for their thermodynamic stability, in particular dispersions of colloidal particles with orientationally and positionally ordered structures [1–5]. These emulsions can be regarded as model systems for the research of quenched disorder effects in partially ordered matter [6–9]. A common feature encountered in these systems is the aggregation of colloidal particles and/or phase separation driven by the fluid medium anisotropy in the ordered mesophase. This results either in a formation of stable superstructures or in expulsion of the particles from the emulsion [2,3] The latter scenario is typically overcome by treating the surface of colloidal particles with an appropriate surfactant. An intriguing behavior has been reported on a homogeneous mixture of didodecyldimethylammonium bromide (DDAB) surfactant-stabilized nanometer-sized water droplets (inverse micelles) in thermotropic liquid crystal 5CB [1]. It was claimed for this system that it exhibits a stable, optically transparent liquid crystalline state, denoted as "transparent nematic phase," which on scales of several nm possesses local nematic order. It was proposed on the basis of optical observations and differential scanning calorimetry (DSC) that on cooling the described system exhibits two distinct phase transformations. First, a transition from the isotropic (I) to a transparent nematic (TN) phase takes place. On further cooling by about 2 K, a phase separation takes place, resulting in a coexistence of bulk nematic (N) and TN phases.

Demixing of micelles from the bulk nematic phase was observed in recent dynamic light scattering [10] and x-ray [11] studies; a fast motion component attributed to paranematic LC fluctuations and a slow motion contribution attributed to scattering by micelles have been detected via the analysis of light intensity autocorrelation function. By comparing the intensity of the two spatially separated components the study was able to identify two distinct phases—a denser micelle-poor nematic phase and a micelle-rich transparent phase with suppressed paranematic fluctuations, thus characterized as isotropic rather than transparent nematic phase.

In this study we offer some additional insight on the nature of the above mentioned phase transition and the accompanying phase separation. We employ quadrupole perturbed deuteron nuclear magnetic resonance (DNMR) spectroscopy and one-dimensional (1D) microimaging. With this approach we confirm the picture of a phase separation into micelle-poor nematic and micelle-rich isotropiclike transparent (subsequently called isotropic) phase. NMR microimaging techniques have been applied before for imaging of emulsions and colloidal systems [12–14]. Here we demonstrate the usefulness of DNMR microimaging experiment for a spatial mapping of nematic and isotropic phases as well as the density profiles of micelles. Our experiments are further supported by optical microscopy and high resolution calorimetry. We also analyze the temperature dependence of the DNMR isotropic spectral component in terms of motional narrowing, induced by translational diffusion of LC molecules among orientationally disordered domains, in order to confirm or reject the proposed transparent nematic state scenario.

II. EXPERIMENTAL PROCEDURES

We prepared nematic microemulsions using the same preparation method as described in [1,9], with micellar size of 4 nm set by the 85% weight percent concentration of

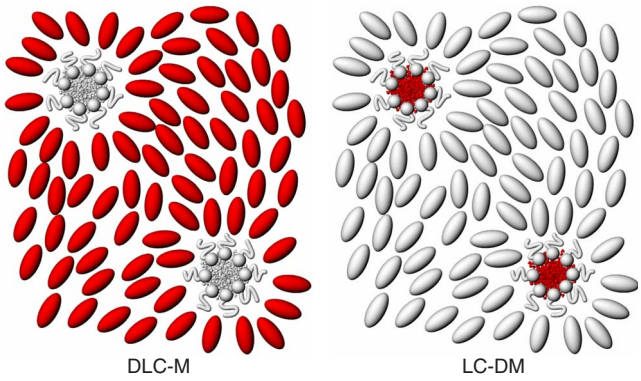

FIG. 1. (Color online) Schematic drawing of the two types of deuterium-labeled microemulsions. The deuterium-labeled component is shown in red (dark) color. DLC-M samples have deuterium labeled liquid crystal, whereas LC-DM samples contain micelles that were prepared with heavy water.

DDAB surfactant in water. We varied the weight ratio ϕ of micelles in 5CB liquid crystal. 10% of 5CB molecules were deuterated at their α positions, thus providing for DNMR sensitivity. Three samples were prepared, with $\phi=0.05$, 0.08, and 0.15, denoted as DLC-M05, DLC-M08, and DLC-M15. We also prepared micellar mixture in which water was replaced with heavy water. A sample in which only micelles were deuterium labeled was prepared from this mixture and nondeuterated 5CB (LC-DM15, $\phi=0.15$). The two complementarily deuterium-labeled samples are shown in Fig. 1. All mixtures were homogenized by stirring in the isotropic phase at $T\approx 330$ K. Samples were filled into glass tubes with an inner diameter of 4.3 mm and a length of about 12 mm and sealed with epoxy glue. Prior to a start of every measurement, each sample was additionally homogenized by shaking the sample container in $T=330$ K water bath. This provided (as verified with NMR microimaging) for adequately homogenized distribution of micelles over the sample independent from the sample's thermal history. Hereafter, we shall call such a sample a "virgin" sample.

The DNMR spectroscopy as well as the NMR microimaging experiments were carried out in the magnetic field of 9 T, corresponding to deuteron Larmor frequency of 58.34 MHz. For NMR microimaging, a Maxwell pair coil based NMR probe was used, which provided for a gradient of magnetic field with the direction matching that of the spectrometer magnetic field as well as the long axis of the vertically positioned sample container. The magnitude of the magnetic field gradient was calibrated with a "phantom" sample to $G=0.09$ T/m, with variations smaller than 0.01 T/m across the space occupied by the largest of the measured samples. We used the solid echo pulse sequence $(90^\circ_x-\tau-90^\circ_y-\tau)$ with the exorcycle phase scheme [15]. The length of the 90° pulse was about 6 μs in spectroscopic experiments and 13 μs in the imaging experiment, whereas τ was 40 μs in both cases. Spectra were first recorded on cooling the virgin sample from the isotropic phase with 500 mK/h rate down to about 20 K below the nominal transition temperature $T^{v}_{\mathrm{I}\to\mathrm{N}}$, at which the nematic phase first appears. The sample was subsequently kept at this low temperature for 8 hours and then heated up with 500 mK/h rate up to about 15 K above $T_{\mathrm{N}\to\mathrm{I}}$. Let us note that $T_{\mathrm{N}\to\mathrm{I}}$, i.e., the temperature of a disappearance of nematic phase on heating, is substantially higher than $T^{v}_{\mathrm{I}\to\mathrm{N}}$. A second cooling run with equal cooling rate was performed after 24 hours of retaining the isotropic state at $T\approx T_{\mathrm{N}\to\mathrm{I}}+15$ K without rehomogenizing the sample.

After each completed NMR investigation on a particular sample, we reproduced the environment and experimental conditions of NMR measurements outside of the magnet and recorded pictures of the sample with a digital camera. The sample tube was, just as in the case of NMR experiments, positioned vertically inside a vacuum glass tube. The temperature, controlled by blowing nitrogen gas across a built-in heater, was stable to within ± 0.2 K. Care was taken to match the calibration of the NMR thermometer and the external thermometer. In accordance with NMR experiments, three runs were performed: A cooling run, a heating run, and a second cooling run with the same cooling and/or heating rates and timings as in the case of NMR experiments. Photographs were taken every 6 minutes corresponding to a temperature change of 0.05 K, with a resolution of 0.01 mm per pixel.

Heat-capacity data were acquired by an automatically operated calorimeter, capable to operate in ac as well as in relaxation mode. The latter, also known as nonadiabatic scanning mode, is sensitive to the latent heat and thus allows for a quantitative estimation of the discontinuous jump in the enthalpy H due to the first-order phase conversion. Detailed description of the technique is given in Refs. [16,17]. The sample, which is contained in a sealed silver cell, was thermally linked to a temperature-stabilized bath (within 0.1 mK) by support wires and by air. The data were collected in three subsequent runs (a cooling run, a heating run, and a second cooling run), thus in a similar fashion and with identical cooling and/or heating rates as in the case of NMR experiments. The mass of the sample was around 40 mg.

III. EXPERIMENTAL RESULTS AND DISCUSSION

In Fig. 2 we show a comparison of NMR spectra for pure 5CB and DLC-M05 recorded at temperatures close to the isotropic-nematic transition ($T_{\mathrm{NI}}=307$ K for bulk 5CB and $T^{v}_{\mathrm{I}\to\mathrm{N}}=304.5$ K for DLC-M05). Above the transition temperature, we observe a single narrow spectral line in both samples. This line corresponds to the isotropic phase in which the fast molecular motion completely averages out the quadrupolar interactions of deuterium nuclei. In the nematic phase, a characteristic doublet is observed, with a splitting $\Delta\nu$ proportional to the local nematic order parameter S,

$$\Delta\nu=\tfrac{3}{4}\nu_q\, S(3\cos^2\theta-1). \qquad (1)$$

Here $\nu_q\approx 60$ kHz is the average quadrupole coupling constant and θ denotes the angle between the liquid crystal director and magnetic field direction. In a strong magnetic field the nematic director is aligned along the field, thus $\theta=0$.

A notable difference between pure 5CB and DLC-M05 is the width of the temperature region, in which the isotropic and nematic phases coexist. Unlike in 5CB, where the coex-

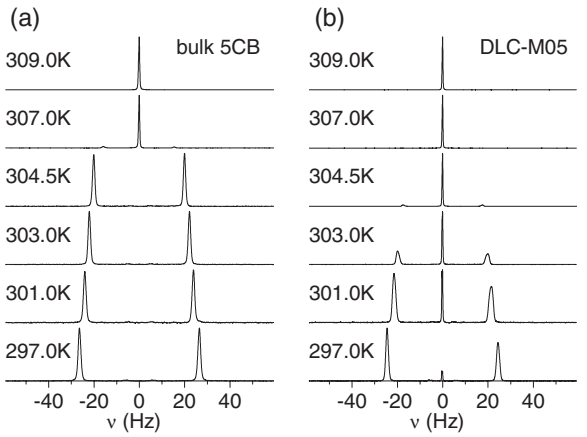

FIG. 2. Selection of NMR spectra for bulk deuterated 5CB (a) and DLC-M05 sample (b). In addition to a decrease of the I-N transition temperature, the microemulsion spectra also exhibit a broad coexistence temperature interval of isotropic and nematic phases.

istence interval is only several tenths of Kelvin, in the microemulsion samples the isotropic LC phase persists down to temperatures more than 20 K below the transition. The temperature dependencies of the relative ratios of the isotropic phase in the three DLC-M samples, as calculated from the line intensities in the respective NMR spectra, are shown in Fig. 3. Also shown in Fig. 3 is a comparison of the temperature dependencies of the nematic doublet splittings, proportional to the nematic order parameter. The presence of micelles slightly diminishes the order parameter in microemulsions as compared to bulk liquid crystal. Higher micelle concentration results in a broader coexistence range, i.e., a more gradual transformation from the isotropic to the nematic phase.

The downward shifts of transition temperatures $T^{v}_{\mathrm{I}\rightarrow\mathrm{N}}$ with respect to T_{NI} of 5CB amount to 2.5 K, 7.2 K, and 13 K for DLC-M05, DLC-M08, and DLC-M15, respectively. They

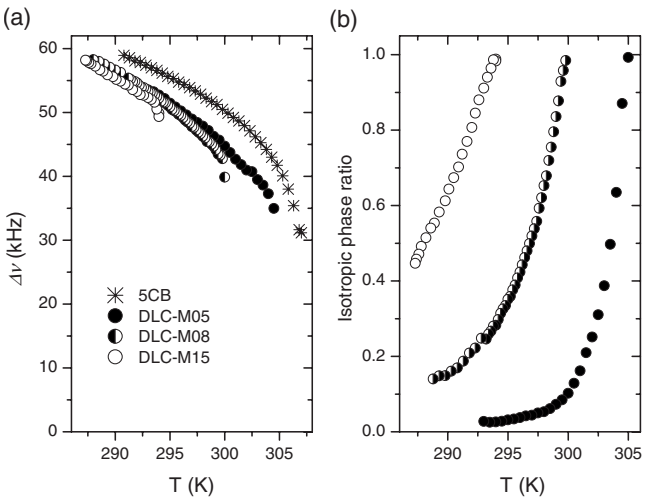

FIG. 3. Temperature dependencies of the frequency splitting of the nematic doublet (a) and of the isotropic phase relative signal intensity (b). For comparison, the temperature dependence of the nematic doublet splitting of pure 5CB is also displayed.

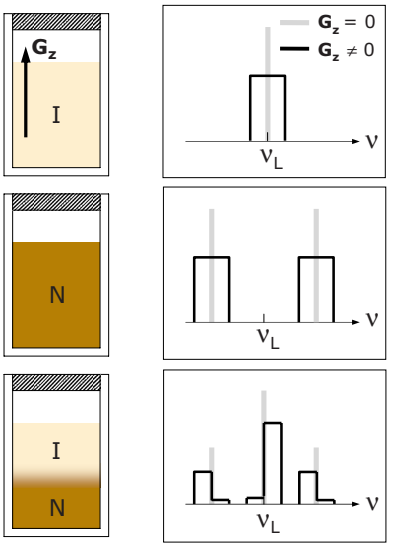

FIG. 4. (Color online) A schematic comparison of theoretical NMR spectra (gray) and spectra with spatially encoded frequencies acquired through NMR microimaging (black) of the deuterated liquid crystal. Three cases are displayed: Isotropic phase, nematic phase, and a system where isotropic and nematic phase coexist and are spatially separated.

obey the $\phi^{2/3}$ dependence on micelle concentration ϕ, as predicted for elastic distortions of the spatially randomly frozen nematic director fields [17]. A difference in the proportionality constant with respect to the diagram presented in [1] may be indicative of differences either in micelle sizes, originating from a possible mismatch in the surfactant to water ratio, or in sample preparation conditions.

Important differences between the phase-transition behavior of bulk liquid crystal and microemulsion samples are observed from density profiles acquired through NMR microimaging. When NMR spectra are recorded in the presence of uniform magnetic field gradient in the z direction (further on we will refer to them as to "microimaging spectra"), a density profile in this direction of the observed (labeled) component is obtained. In such a case, nuclei in molecules situated at different z coordinates within the container experience different magnetic field and resonate at different, spatially encoded frequencies. Thus, the shape of a particular spectral line in the presence of the microimaging gradient reflects the density profile of the labeled component (LC molecules or micelles).

When observing deuterated liquid crystal, information on the type of LC phase is also obtained in addition to the spatial density profile. This is so since in the respective spectra, isotropic and nematic phases can clearly be resolved (sharp central line vs nematic doublet). This is illustrated in Fig. 4. If the gradient is perfectly uniform across the volume, occupied by the sample, the otherwise narrow NMR spectral lines broaden into rectangularly shaped lines. The spatial separation of the nematic and isotropic phase components is observed as a narrowing of these rectangular lines. For instance, the narrowing of the nematic doublet towards lower frequencies corresponds to the accumulation of the nematic phase at the bottom of the container. Likewise, the narrowing

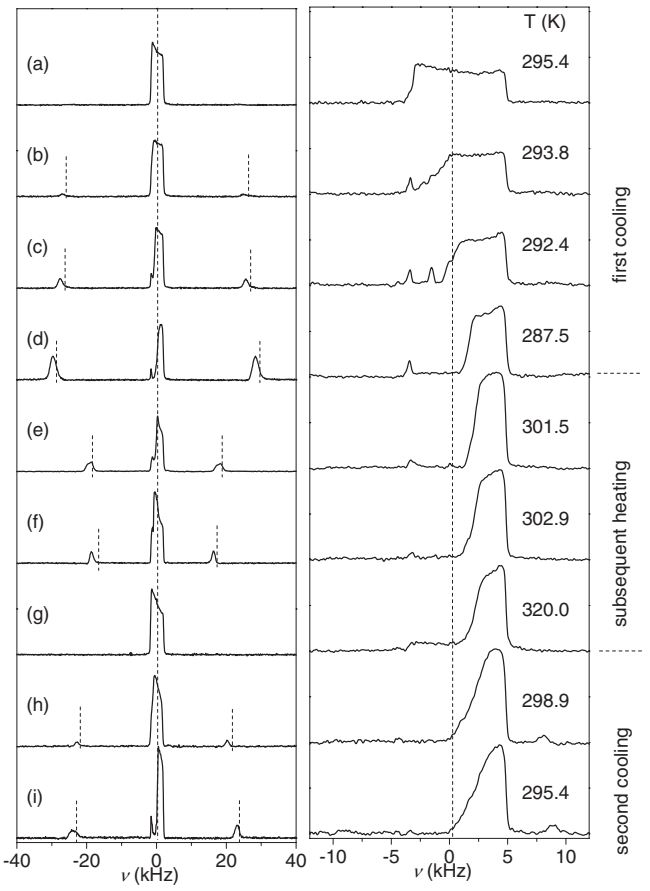

FIG. 5. DLC-M15 and LC-DM15 sample NMR microimaging spectra recorded at heating and/or cooling runs at temperatures matching those of Fig. 6. DLC-M15 spectra display the density profile of isotropic and nematic components, while LC-DM15 spectra display the density profile of micelles. The dashed lines mark the center of the sample container.

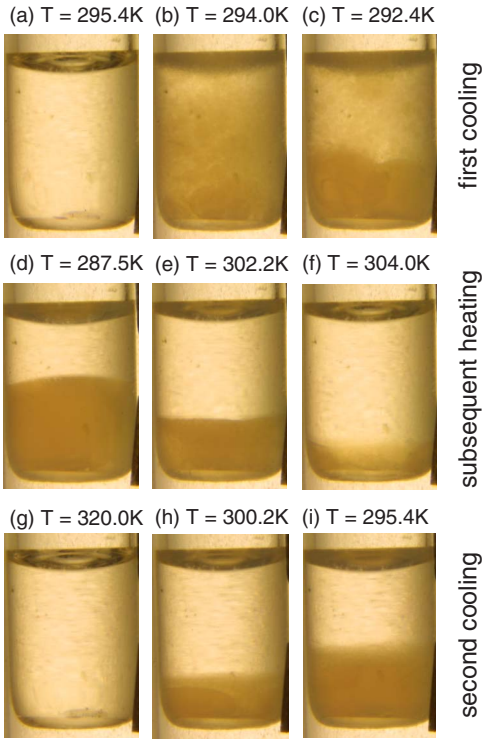

FIG. 6. (Color online) Representative photographs of the DLC-M15 sample showing an irreversible phase-transition-driven separation of components on cooling (a)–(d), hysteretic melting of the nematic phase on heating (d)–(g), and a second cooling run that is almost a mirror picture of the heating run (g)–(i). Corresponding DLC-M15 as well as LC-DM15 sample NMR microimaging spectra at matched temperatures are shown in Fig. 5.

of the isotropic "rectangle" towards higher frequencies corresponds to the accumulation of the isotropic part at the top of the container.

The relation between the z coordinate of the imaged volume and its resonance frequency is linear. In our case a slice with a height (z coordinate) of one millimeter is mapped to an approximately 600 Hz wide interval in the respective microimaging spectrum. The spatial resolution is slightly reduced by intrinsic (homogeneous and inhomogeneous) line broadening. This is particularly noticeable for the nematic doublet lines, whose linewidth in the absence of gradient lies just below 1 kHz. The effect is less pronounced for the central isotropic line. Its linewidth (less than 300 Hz) contributes no more than 0.25 mm to the error of z-coordinate determination.

Figure 5 shows a selection of consequently recorded microimaging spectra of the DLC-M15 and LC-DM15 samples during the combined cooling-heating-cooling run. Each spectral pair is supported by an identically labelled photograph of the sample in Fig. 6. The DLC-M15 spectra exhibit the density profile of the two liquid crystal phases, whereas the LC-DM15 spectra reflect the micellar density profile. All spectra are shown with normalized intensities. Prior to recording a NMR microimaging spectra at a particular temperature, conventional NMR spectra in the absence of gradient were recorded in order to set the reference for the center of the sample container.

Figure 5(a) of the LC-DM15 sample best demonstrates that in the virgin sample, micelles are uniformly distributed across the sample. When, on cooling, $T^{v}_{\mathrm{I}\rightarrow\mathrm{N}}$ is reached, the microemulsion sample becomes turbid [Fig. 6(b)]. Already at this point, as visible in the spectrum of LC-DM15 sample in Fig. 5(b), the micelles start migrating from the bottom part of the container to the upper part. On further cooling a macroscopic phase separation takes place. The denser opaque nematic component gathers at the bottom of the container in the form of droplets, which upon further cooling agglomerate [Figs. 5(c) and 6(c)]. The transparent isotropic component is pushed towards the top due to its smaller specific weight. The micelles seem to already at this stage be completely expelled from the nematic phase and only present in the isotropic component of the liquid crystal. As the sample temperature is further decreased, the relative ratio of the micelle-rich isotropic phase at the top diminishes on the account of the formation of opaque micelle poor nematic phase component at the bottom of the container [Figs. 5(d) and 6(d)].

Notably, the course of events observed with a virgin sample is neither reproduced on heating the sample back from the nematic phase nor on a second cooling run. As on heating the temperature rises, the interface between the two

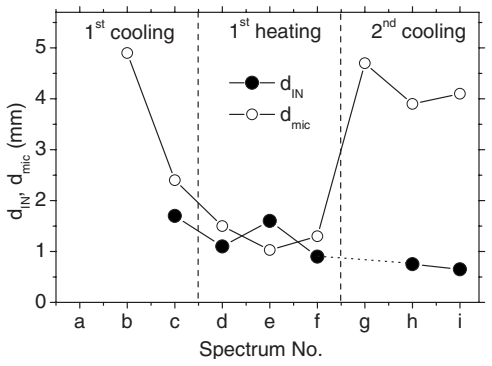

FIG. 7. Evolution of the width of the phase boundary of isotropic and nematic components (d_{IN}, DLC-M15 sample) and the transition region between micelle-rich and micelle-poor region (d_{mic}, LC-DM15 sample). These widths, extracted from the NMR microimaging spectra (Fig 5), correspond to intervals over which the signal of a particular component rises from 15% to 85% of its maximum spectral intensity.

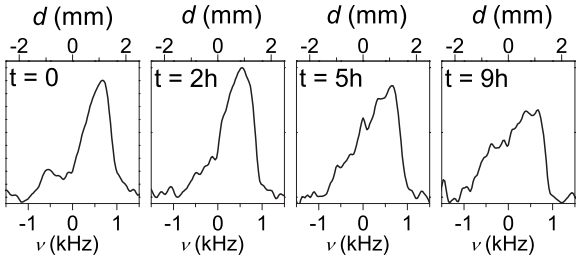

FIG. 8. NMR microimaging spectra of a "thin" LC-DM15′ sample recorded at times 0, 2 h, 5 h, and 9 h after a phase-separated sample had been suddenly heated to 320 K. Deuterium-labeled micelles are thermally redistributed across the sample (2.5 mm height) within approximately 1 day.

coexisting, spatially separated phases, moves towards the bottom of the container, since the nematic phase at the bottom is converted into the isotropic phase on the top [Figs. 5(e), 5(f), 6(e), and 6(f)]. The nematic component completely disappears at $T_{N\to I}$ [Fig. 5(f) and 6(f)], which is close to T_{NI} of bulk 5CB. This is consistent with the finding that the nematic phase at the bottom contains micelles in very small concentration.

After having the sample held at 320 K for 24 hours [Fig. 6(g)], only a small part of micelles (about 10%) diffuse back to the lower part of the container [see DLC-M spectrum in Fig. 6(g)]. On repeated cooling, however, these micelles are expelled back to the upper part of the container, as nematic phase builds up gradually (i.e., without any turbid appearance) from the bottom [Figs. 5(h), 5(i), 6(h), and 6(i)]. The nematic phase appears at temperature $T_{I\to N}$, which almost matches $T_{N\to I}$. This behavior is a reversed picture of the previously performed heating run and so are any subsequent heating and cooling runs.

The isotropic (central) spectral parts of DLC-M spectra in Fig. 5 clearly demonstrate that the interface between the isotropic and nematic component is relatively sharp, whereas the micellar concentration profile is more gradual (LC-DM spectra in Fig. 5). The two characteristic widths d_{IN} and d_{mic} of the isotropic-nematic and micelle-poor-micelle-rich transition regions, respectively, are shown in Fig. 7. When heating a phase-separated sample, d_{mic} reaches about 5 mm. Nevertheless, the isotropic-to-nematic interface remains very sharp (about 0.6 mm) (Fig. 7). A detailed comparison of the density profiles and photographs of individual compounds and phases in both samples leads to a conclusion that micelles, in a given experimental geometry, do not remix back into the nematic component.

The above described cooling-heating-cooling experiment was repeated with "thin" samples, whose vertical dimensions were smaller than d_{mic}. The "thin" samples, denoted as DLC-M15′ and LC-DM15′, were prepared in the same way as the DLC-M15 and LC-DM15, except for their reduced height of about 2.5 mm. At the first cooling run of the virgin sample, as well as at subsequent heating run, an almost identical behavior and transition temperature were detected as for the "thick" DLC-M15 and LC-DM15 samples. The difference to "thick" samples occurred on subsequent cooling, preceded by a 24-hour heating at 320 K. Here the phase transition occurred at the same temperature as during the first cooling run. Unlike in the "thick" DLC-M15 sample, the nematic component did not start to build-up from the bottom, but the onset of the transition was identical to the first cooling run, i.e., with an overall turbid appearance.

Obviously, within the 24-hour heating period the micelles redistribute uniformly across the "thin" sample, which results in a close-to-virgin sample. We proved this by recording consecutive NMR microimaging spectra of the initially phase-separated LC-DM15′ sample while keeping it at 320 K. These spectra (shown in Fig. 8) were recorded at times 0, 2 h, 5 h, and 9 h after the phase-separated sample had suddenly been heated to 320 K. Evidently, micelles do redistribute in the course of the 24-hour exposure to high temperature in the isotropic phase, in contrast to the thick samples, where irreversible separation of the micelles takes place. An estimate of the diffusion coefficient of the micelles in the isotropic liquid crystal following from the above measurements gives a value between 10^{-11} m^2 s^{-1} and 10^{-10} m^2 s^{-1}, which is of the same order as the diffusion rate of the liquid crystalline molecules themselves [18].

In Fig. 9 we show the results of our calorimetric measurements: The specific heat (C_p) values as a function of temperature for the DLC-M08 sample and pure 5CB, obtained from ac runs on cooling and heating, as well as the $C_{eff}(T)$ from the relaxation run, obtained during the cooling. The C_p anomaly related to the conversion from the isotropic to nematic state of the DLC-M08 sample is suppressed and shifted toward lower temperatures in comparison to bulk 5CB values.

The observed large difference between the relaxation run and the ac run data demonstrates the presence of latent heat in a wide temperature interval, in contrast to pure 5CB where this coexistence range is narrow (several tenths of K) and ends abruptly. This continuous release of latent heat corresponds to continuous conversion of isotropic regions (domains) into nematic ones. The expelling of micelles from the newly formed nematic domains results in an increase of the micellar density of the coexisting isotropic component. Consequently, the I-N transition temperature of the isotropic

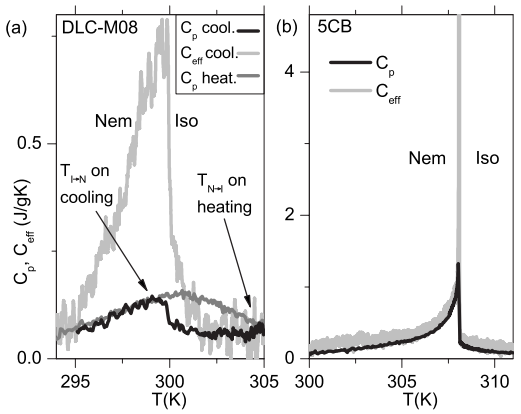

FIG. 9. Temperature dependence of specific heat capacity from ac $[C_p(T)]$ and relaxation $[C_{\mathrm{eff}}(T)]$ calorimetric measurements of (a) DLC-M08 microemulsion and (b) bulk 5CB. Broad temperature range with latent heat release indicated by the smeared peak of $C_{\mathrm{eff}}(T)$ in (a) indicates gradual I-N conversion of regions from which the micelles are expelled. The consequence of the irreversible phase separation process is the mismatch between the cooling and heating run $C_p(T)$ data as well as the difference between $T_{\mathrm{I}\rightarrow\mathrm{N}}$ and $T_{\mathrm{N}\rightarrow\mathrm{I}}$.

component is further lowered, so the above loop repeats at lower temperatures. Because of this gradual I-N conversion one observes a broad anomaly in C_p with a pronounced low-temperature tail. On heating, the micelles from the top, micelle-rich layer, diffuse back into the N phase, effectively lowering the I-N transition temperature at the I-N interface, thus accelerating the melting of the adjacent nematic regions. Again, this gradual remixing process results in a broad C_p anomaly observed on heating (see Fig. 9). The high-temperature specific heat tail extends almost to the $\mathrm{T_{NI}}$ of bulk 5CB, demonstrating the existence of almost micelle-free nematic domains. A subsequent second cooling run, preceded by an intermediate 24-hour heating period at 320 K, resulted in a $C_p(T)$ dependence that is identical to that of the first cooling run. This indicates that reheating makes the sample close to virginlike, i.e., that the micelles almost completely remix in the liquid crystal. Indeed, this is consistent with the findings of NMR microimaging experiments in "thin" samples (note that the thickness of the calorimetric cells is about 1 mm). The outcomes of the calorimetric study on similar 8CB microemulsions [9] and of the present study match very well in confirming the above-presented scenario of micellar phase separation.

Let us now focus our attention to the nature of the micelle-rich isotropiclike phase component of the investigated microemulsion, until now referred to as the "isotropic phase." In Ref. [1] it was proposed that even at temperatures about 2 K above $T^{v}_{\mathrm{I}\rightarrow\mathrm{N}}$, local nematic order is established in domains with sizes of the order of the intermicellar distances and that this type of ordering persists in the phase-separated, optically transparent nematic component. For confinement sizes of several nm, the external magnetic field of several Tesla cannot align the nematic director, since the magnetic coherence length exceeds the confinement size for at least one order of magnitude [19]. A transparent nematic phase thus exhibits an isotropic distribution of nematic directors and, consequently, yields a powderlike DNMR spectrum, given that no molecular translational diffusion takes place. However, even a moderate molecular translational diffusion results in a strong spectral averaging in LC systems, whenever nematic director is strongly spatially modulated, as indeed is the case for the proposed transparent nematic phase scenario [20]. In the case of unhindered isotropic reorientations, this so-called RMTD (reorientations mediated by translational displacements) mechanism averages the powder spectrum into a Lorentzian-shaped line with a full width at half-maximum of $W=1/5\pi\nu_q^2S^2\tau$ [18,21]. For RMTD's, τ can be related to translational diffusion coefficient D via $\langle r^2\rangle=6D\tau$. Here $\langle r^2\rangle$ represents a mean-square distance of the variation in nematic director's orientation. By approximating this distance with the intermicellar distance l we obtain

$$W_{\mathrm{TN}}=\frac{\pi\nu_q^2S^2l^2}{30D}=CS^2l^2. \tag{2}$$

Here TN stands for "transparent nematic." The anomaly in $S(T)$, associated with the proposed onset of transparent nematic state with nonzero S, should therefore result in a linewidth broadening of $W_{\mathrm{TN}}(T)$. Experimentally determined value of the diffusion constant is $D\approx5\times10^{-11}$ m^2 s^{-2} in bulk 5CB and decreases with decreasing confinement size ($D\approx8\times10^{-12}$ m^2 s^{-2} in 7.5 nm controlled-pore glass) [18]. With an estimate $D=10^{-11}$ m^2 s^{-2}, the proportionality constant in Eq. (2) amounts to $C=38$ Hz nm^{-2}. The intermicellar distances are given by $l=a(4\pi/3\phi)^{1/3}$, where $a=2$ nm is the radius of the inverse micelles [1]. They amount to 6 nm, 7.5 nm, and 9 nm for the DLC-15, DLC-08, and DLC-05 sample, respectively. In the case of ideal orientational ordering, $S=1$, the linewidth broadenings, obtained by inserting these values into Eq. (2), are $W_{\mathrm{TN}}\approx1.3$ kHz, 2.1 kHz, and 3 kHz. However, in the TN phase, the nematic order parameter values are expected to be lower than the values in bulk 5CB ($S\approx0.3$ at T_{NI}). Due to a quadratic power dependence of W_{TN} on S, the actual widths are at least one order of magnitude smaller than the ones stated above. Specifically, a transparent nematic phase with intermicellar distance of $l=7.5$ nm and nematic order of $S=0.2$ should give rise to a $W_{\mathrm{TN}}\approx90$ Hz linewidth broadening. This relatively small broadening is comparable to the pretransitional broadening $W_{\text{pre-t}}(T)$ originating from the surface-induced ordering of LC molecules in confined systems [18], as well as to the relatively high inhomogeneous broadening of spectral lines due to magnetic field inhomogeneity ($W_0\approx175$ Hz). In a real experiment, the total linewidth $W=W_0+W_{\text{pre-t}}(T)+W_{\mathrm{TN}}(T)$ is measured. Results for DLC-08 and DLC-15 are shown in Fig. 10. We note that with decreasing micelle concentration, $W(T)$ points become more scattered, up to the point of preventing successful measurement (DLC-05 sample). We accredit these problems to the separation of micelles out of the nematic phase and possible aggregation of micelles in the micelle-rich isotropic phase. Within the experimental error, the measured temperature dependencies of Fig. 10 reveal no anomaly, i.e., no first-order-type discontinuity, characteristic for the onset of nematic order detectable via the $W_{\mathrm{TN}}(T)$ term. $W(T)$ rather exhibits a continuous in-

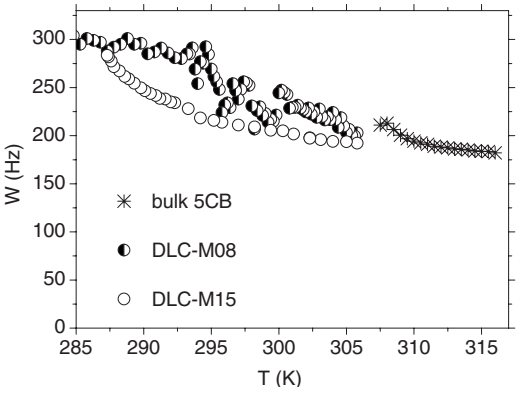

FIG. 10. Temperature dependence of the full width at half-maximum of the central "isotropic" DNMR spectral line for bulk 5CB and DLC-M samples.

crease with decreasing temperature over a large temperature interval, deep into the nematic phase, far beyond the temperature range of the proposed TN phase. The observed monotonous profile signifies that the $W(T)$ dependence is solely controlled by thermally activated, Arrhenius-type diffusion coefficient $D(T)$ [Eq. (2)]. Moreover, the pronounced increase in $W(T)$ at lower temperatures for the DLC-M15 samples can be attributed to the surface order term $W_{\text{pre-t}}$ [18], related to the establishment of nematic order at the surface of micelles with homeotropic anchoring conditions [1]. Therefore, measurements of the DNMR linewidths of the isotropic spectral component do not support the hypothesis on the existence of transparent nematic phase in DLC microemulsions with nematic order parameter values comparable to values found in bulk nematic phases. If a transparent nematic phase exists, the respective S does not exceed the surface-induced values of S, typically 0.01–0.1.

IV. CONCLUSIONS

We have developed an NMR method for selective imaging of the density profile of ordered (nematic) and isotropic liquid crystal phases as well as of water-in-oil micelles in DLC nematic microemulsions. This method is used to clearly demonstrate the separation of micelles from the nematic phase, resulting in a coexistence of micelle-poor nematic phase and micelle-rich isotropic phase over a broad temperature interval. Thermal remixing of the phase-separated micelles is an extremely slow process, of the order of several days even at temperatures high above T_{NI} of bulk 5CB. Our findings on the phase-separation process are supported by the results of high resolution ac-calorimetric experiments and are in agreement with results of the ac-calorimetric study of similar microemulsions based on 8CB smectic liquid crystal, in which the sharp second-order nematic-smectic-A transition was used to sensitively probe the interplay between the liquid crystal and the inverse micelles. The optically transparent phase, which coexists with the nematic phase, is observed as an isotropic, Lorentzian-shaped peak in the DNMR spectrum. The temperature profile of its linewidth is similar to that of a conventional isotropic phase of confined LC systems. No spectral anomalies, reminiscent of the proposed formation of an intermediate, transparent nematic phase, have been detected. This either proves that such a phase is not thermodynamically stable due to elastic forces-driven separation of inverse micelles from nematic domains, or that the nematic order in a transparent nematic phase is extremely low. Due to a relatively high surface-to-volume ratio of the liquid crystal component in our microemulsions, it is extremely difficult to resolve between the possible bulk transparent nematic order and the surface-induced order. In order to provide for a definite answer on the existence of the transparent nematic phase, an experimental method capable of determining small nematic order parameter values on the spatial scale of only several nm needs to be employed.

Let us note that it was very recently found by Tanaka and his collaborators [22] that there are two distinct states of 5CB-DDAB-water mixtures. One is an equilibrium stable state composed of uniform inverse micelles, whereas the other is a metastable, but very long-lived state with inverse micelles and larger micelles (about 100 times larger than the inverse micelles), which was confirmed by dynamic light scattering measurements. Only the latter has the TN phase, whereas the former does not. It was confirmed [22] that a one-step mixing (mixing 5CB, DDAB, and water all together at once), which is used in Ref. [10], always results in a stable phase without the TN phase. This is consistent with what was reported in Ref. [10]. Which of these two states is realized obviously depends on the details of the sample preparation. Considering this, the absence in the present study of the spectral anomaly expected for the TN phase implies one of the following three scenarios: (i) the particular samples used here do not possess the TN phase; (ii) although the TN phase exists in the samples, its order parameter is too small to be resolvable with NMR, as reasoned above; (iii) there is no bulk transparent nematic order in the investigated system, and the transparent phase is just a normal isotropic phase with (highly concentrated) inverse micelles. To draw a more definite conclusion, further investigations thus need to be performed.

[1] J. Yamamoto and H. Tanaka, Nature (London) **409**, 321 (2001).
[2] C. Pizzey, J. V. Duijneveldt, and S. Klein, J. Phys.: Condens. Matter **16**, 2479 (2004).
[3] J.-C. Loudet, P. Barois, and P. Poulin, Nature (London) **407**, 611 (2000).
[4] P. Poulin, H. Stark, T. Lubensky, and D. Weitz, Science **275**, 1770 (1997).
[5] I. Muševič, M. Škarabot, U. Tkalec, M. Ravnik, and S. Žumer, Science **313**, 954 (2006).

[6] T. Bellini, N. A. Clark, V. Degiorgio, F. Mantegazza, and G. Natale, Phys. Rev. E **57**, 2996 (1998).
[7] M. Caggioni, A. Roshi, S. Barjami, F. Mantegazza, G. S. Iannacchione, and T. Bellini, Phys. Rev. Lett. **93**, 127801 (2004).
[8] G. Cordoyiannis, G. Nounesis, V. Bobnar, S. Kralj, and Z. Kutnjak, Phys. Rev. Lett. **94**, 027801 (2005).
[9] Z. Kutnjak, G. Cordoyiannis, G. Nounesis, A. Lebar, B. Zalar, and S. Žumer, J. Chem. Phys. **122**, 224709 (2005).
[10] T. Bellini, M. Caggioni, N. A. Clark, F. Mantegazza, A. Maritan, and A. Pelizzola, Phys. Rev. Lett. **91**, 085704 (2003).
[11] G. Toquer, G. Porte, M. Nobili, J. Appell, and C. Blanc, Langmuir **23**, 4081 (2007).
[12] F. P. Duval, P. Porion, and H. V. Damme, J. Phys. Chem. B **103**, 5730 (1999).
[13] K. G. Hollingsworth and M. L. Johns, J. Colloid Interface Sci. **296**, 700 (2006).
[14] M. A. d'Avila, N. C. Shapley, J. H. Walton, R. J. Phillips, S. R. Dungan, and R. L. Powell, Phys. Fluids **15**, 2499 (2003).
[15] J. H. Davis, K. R. Jeffrey, M. Bloom, M. I. Valic, and T. P. Higgs, Chem. Phys. Lett. **42**, 390 (1976).
[16] H. Yao, K. Ema, and C. W. Garland, Rev. Sci. Instrum. **69**, 172 (1998).
[17] Z. Kutnjak, S. Kralj, G. Lahajnar, and S. Žumer, Phys. Rev. E **68**, 021705 (2003).
[18] M. Vilfan, T. Apih, A. Gregorovič, B. Zalar, G. Lahajnar, S. Žumer, G. Hinze, R. Bohmer, and G. Althoff, Magn. Reson. Imaging **19**, 433 (2001).
[19] J. W. Doane, in *Magnetic Resonance of Phase Transitions*, edited by F. J. Owens, C. P. Poole, and H. A. Farach (Academic, New York, 1979).
[20] F. Grinberg and R. Kimmich, Magn. Reson. Imaging **19**, 401 (2001).
[21] A. Abragam, *Principles of Nuclear Magnetism* (Oxford University Press, New York, 1961).
[22] M. T. M. Nogawa, R. Nishida, and H. Tanaka (unpublished).